Maximum Observation of a Faster Non-Maneuvering Target by a Slower Observer

Isaac E. Weintraub[1], Alexander Von Moll[2], Eloy Garcia[2], David Casbeer[2],
Zachary J. L. Demers[1], and Meir Pachter[3]

***Abstract*— This paper considers a two agent scenario containing an observer and a non-maneuvering target. The observer is maneuverable but is slower than the course-holding target. In this scenario, the observer is endowed with a nonzero radius of observation within which he strives at keeping the target for as long as possible. Using the calculus of variations, we pose and solve the optimal control problem, solving for the heading of the observer which maximizes the amount of time the target remains inside the radius of observation. Utilizing the optimal observer heading we compute the exposure time based upon the angle by which the target is initially captured. Presented, along with an example, are the zero-time of exposure heading, maximum time of observation heading, and proof that observation is persistent under optimal control.**

I. Introduction

Intelligence, Surveillance, and Reconnaissance (ISR) missions have been of great interest to the aerospace community [1]–[4]. One goal of an ISR platform is the observation of a target, whether it be moving or stationary. In this paper we consider the observation of a faster but non-maneuvering target by a slower observer.

The task of observation of slower ground targets by an aerial platform were considered in [5]–[7]. In [5], a quad-rotor utilizing a downward-pointing camera tracks a ground vehicle restricted to a road network. In [6], an ISR platform equipped with a gimbaled camera was considered, thus allowing the ISR platform to observe a ground target at various aspect angles. Similarly, Skydio, a startup company aimed at personal unmanned air platforms, has considered a quad-rotor aircraft for persistent surveillance of a mobile ground target [7]. The quad-rotor platform performs persistent surveillance and obstacle avoidance in order to recording a designated mobile target.

While this paper considers a single observer and single target, another has considered proximity based capture [8]. In [8], the pursuit-evasion game was terminated when the pursuer and evader were within a defined proximity, this work aims to consider how proximity can be maintained after capture. Other works have considered coordinated observers tasked with identifying a single mobile target [9], [10]. In [9], sensor coverage effectiveness for a single mobile target and a group of mobile sensors was investigated. In their work, the authors showed the connection between numbers of searchers, the amount of searcher motion, and how that trade-off was dependent on the amount of motion for the searcher relative to the target. In [10], the coverage of a mobile sensor network resulting from continuous movement of sensors was studied. In their work, the authors took a game theoretic approach and obtained the optimal mobility strategy for sensors and intruders.

Investigation of differential games concerning the surveillance of an evading agent were considered in [11]–[16]. In these differential games a pursuer with a detection region was pitted against an evader whose goal was to escape as soon as possible. The differential game studied by Dobbie and Taylor considered a fast pursuer with turn restrictions and circular surveillance region against a slower maneuverable evader capable of instantaneous changes in heading [11], [12]. Different to Taylor's work, Lewin imposed a turning rate constraint on the pursuer and allowed the pursuer's speed to vary from full stop to a bounded maximum [13], [14]. Another differential game investigated by Fuchs involved a fast pursuer with radar cross section was pitted against a slower and less maneuverable evader [15]. In the game, the pursuer strives to accumulate enough information about the target to achieve a defined probability of identification while the evader tries to evade the pursuer to remain undetected.

A closely related work by Garnett and Flennner is presented in [17]. In their work a model for maximal information sharing between UAVs was posed and solved utilizing optimal control. Also, the ISR platform was faster than the targets being tracked and a polar function was utilized to model sensor effectiveness. Because of model complexity they required the use of a nonlinear program solver to numerically find the optimal control which maximized the sensing problem.

While the previous works have described optimal means of conducting ISR missions when the ISR platform is faster than the target, less common is the consideration of conducting ISR on targets which are faster. In an early work by Breakwell, a pursuit-evasion game was posed wherein a slower pursuer was employed against a faster evader [18]. Breakwell, also considered a nonzero capture radius for the slower pursuer. The approach taken by Breakwell solved for the acquisition of a faster evader by a slower pursuer, but ISR requires keeping the pursuer within the surveillance range of the pursuer for as long as possible.

[1]Air Force Research Laboratory (AFRL/RQQD), Wright-Patterson AFB, OH 45433, USA isaac.weintraub.1@us.af.mil, zachary.demers@us.af.mil

[2]Control Science Center of Excellence, Air Force Research Laboratory, Wright-Patterson AFB, OH 45433, USA alexander.von_moll.@us.af.mil, david.casbeer@us.af.mil, eloy.garcia.2@us.af.mil

[3]Department of Electrical Engineering, Air Force Institute of Technology, Wright-Patterson AFB, OH 45433, USA meir.pachter@afit.edu

Distribution A: Approved for Public Release (Case#:88ABW-2019-4174)

One reason why we consider the target to be faster than the observer is for the modeling of air-to-air ISR missions. In the event that a slower ISR platform has made contact with a faster target, we consider the max-time observation of the faster target, utilizing optimal control theory [19]. This paper poses and solves for the heading of a slower observer which results in max-time observation of the faster target.

II. Optimal Control

Consider the optimal observation of a faster, non-maneuvering target. We define the constant velocities of the observer (O) and the target (T) as v_O and v_T respectively. The complete state of the observation scenario is:

$$\mathbf{x} = [x_O, y_O, x_T, y_T] \in \mathbb{R}^4$$

where (x_O, y_O) and (x_T, y_T) are the positions of O and T respectively. Consider motion to be restricted to the 2-D plane, commonly found in pursuit-evasion scenarios of Isaacs [20]. The observer's control variable is his instantaneous heading angle $u_O(t) = \psi(t)$. The equations of motion for the two agent scenario are the following:

$$\begin{aligned} \dot{x}_O &= v_O \cos\psi \qquad \dot{x}_T = v_T \cos\phi \\ \dot{y}_O &= v_O \sin\psi \qquad \dot{y}_T = v_T \sin\phi \end{aligned} \tag{1}$$

where the course of the non-maneuvering target, ϕ, is constant and is known by the observer. The control of the observer is his heading: $\psi \in [0, 2\pi)$. At the onset we consider the target to be a distance R from the observer. Also, the observer is at an aspect angle θ from the target, pictorially shown in Fig. 1. This circular model assumes that observation is independent of the observer's heading. In this paper we consider the time-optimal strategy of the observer, O which maximize the time the fast target is kept under observation.

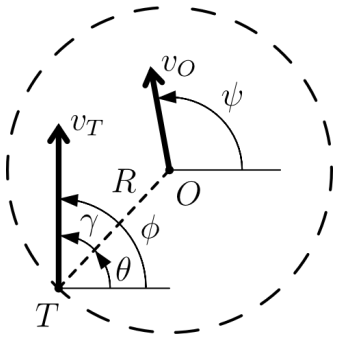

Fig. 1. Initial Engagement Geometry

Without loss of generality, the speed ratio between the observer and the target is defined as: $\alpha = v_O/v_T$. In the scenario, the target is faster than the observer and therefore: $0 < \alpha < 1$. Utilizing the speed ratio parameter, the non-dimensional dynamics in (1) are re-written as follows:

$$\begin{aligned} \dot{x}_O &= \alpha \cos\psi \qquad \dot{x}_T = \cos\phi \\ \dot{y}_O &= \alpha \sin\psi \qquad \dot{y}_T = \sin\phi \end{aligned} \tag{2}$$

Since the target is faster than the observer, escape from the circular observation envelope is guaranteed. Moreover, the termination set which represents the escape of the target from the observation circle is defined as follows:

$$\mathscr{C} = \{\mathbf{x} | R^2 - (x_O - x_T)^2 - (y_O - y_T)^2 \leq 0, t > 0\} \tag{3}$$

The terminal time, t_f, is defined as the instant where the state and time satisfies (3); at which time, the terminal state is: $\mathbf{x}(t_f) = (x_{O_f}, y_{O_f}, x_{T_f}, y_{T_f})$. Since our objective is to maximize the time by which the target remains within the circular observation radius, we consider the max-time objective functional:

$$\min J = \int_0^{t_f} -1 \, dt \tag{4}$$

The optimal time of observation is $t_f^* = \min J$ subject to the termination set in (3). The goal is to find the optimal observer's heading time history which minimizes the objective cost functional in (4), namely:

$$\psi^*(t) = \underset{\psi}{\operatorname{argmin}} J \tag{5}$$

We form the Hamiltonian:

$$\mathscr{H} = \lambda_{x_O} \alpha \cos\psi + \lambda_{y_O} \alpha \sin\psi + \lambda_{x_T} \cos\phi + \lambda_{y_T} \sin\phi \tag{6}$$

where the costates are $\lambda = [\lambda_{x_O} \ \lambda_{y_O} \ \lambda_{x_T} \ \lambda_{y_T}]$.

A. Necessary Conditions for Optimality:

First, we would like to formulate and draw conclusions about the optimal control utilizing the first-order necessary conditions for optimality. Utilizing the Hamiltonian in (6), we may formulate the necessary conditions for optimality:

$$\dot{\mathbf{x}}^*(t) = \frac{\partial \mathscr{H}(\mathbf{x}^*(t), \lambda^*(t), u_O^*(t), t)}{\partial \lambda^*(t)} \tag{7a}$$

$$\dot{\lambda}^*(t) = -\frac{\partial \mathscr{H}(\mathbf{x}^*(t), \lambda^*(t), u_O^*(t), t)}{\partial \mathbf{x}^*(t)} \tag{7b}$$

$$0 = \frac{\partial \mathscr{H}(\mathbf{x}^*(t), \lambda^*(t), u_O^*(t), t)}{\partial u_O^*(t)} \tag{7c}$$

and $\mathscr{H}(t_f) = 0$. Where the superscript, $*$, represents optimally. Evaluating the necessary condition described in (7c):

$$\begin{aligned} 0 =& \frac{\partial}{\partial \psi}(\lambda_{x_T}^* \cos\phi + \lambda_{y_T}^* \sin\phi + \lambda_{x_O}^* \alpha \cos\psi + \lambda_{y_O}^* \alpha \sin\psi) \\ =& -\alpha \lambda_{x_O}^*(t) \sin\psi^*(t) + \alpha \lambda_{y_O}^*(t) \cos\psi^*(t) \\ =& -\lambda_{x_O}^*(t) \sin\psi^*(t) + \lambda_{y_O}^*(t) \cos\psi^*(t) \end{aligned} \tag{8}$$

Bringing the two terms in (8) to either side of the equation, squaring, and using the trigonometric identity $\cos^2\psi^* = 1 - \sin^2\psi^*$, one may obtain the following:

$$\lambda_{x_O}^{*2}(t) \sin^2\psi^*(t) = \lambda_{y_O}^{*2}(t)(1 - \sin^2\psi^*) \tag{9}$$

Through algebraic manipulation of (9) one may obtain the following:

$$\sin^2\psi^*(t) = \frac{\lambda_{y_O}^{*2}(t)}{\lambda_{x_O}^{*2}(t) + \lambda_{y_O}^{*2}(t)} \tag{10}$$

Evaluating the necessary condition in (7b), we have four equations, one for each costate:

$$\dot{\lambda}^*_{x_O}(t) = -\frac{\partial \mathscr{H}(\mathbf{x}^*(t), \lambda^*(t), u^*_O(t), t)}{\partial x^*_O(t)} = 0 \tag{11a}$$

$$\dot{\lambda}^*_{x_T}(t) = -\frac{\partial \mathscr{H}(\mathbf{x}^*(t), \lambda^*(t), u^*_O(t), t)}{\partial x^*_T(t)} = 0 \tag{11b}$$

$$\dot{\lambda}^*_{y_O}(t) = -\frac{\partial \mathscr{H}(\mathbf{x}^*(t), \lambda^*(t), u^*_O(t), t)}{\partial y^*_O(t)} = 0 \tag{11c}$$

$$\dot{\lambda}^*_{y_T}(t) = -\frac{\partial \mathscr{H}(\mathbf{x}^*(t), \lambda^*(t), u^*_O(t), t)}{\partial y^*_T(t)} = 0 \tag{11d}$$

From the necessary conditions in (11) we may infer that the optimal costate trajectories are constant, i.e.: $\lambda^*(t) = \lambda^*$ because the observer is holonomic. Moreover, since the costates are constant, the optimal heading of the observer is constant under optimal play. This result may be derived from (10). Therefore, the resulting optimal trajectory of the observer is a straight-line trajectory:

$$\psi^*(t) = \psi^* = \sin^{-1}\left(\frac{\lambda^*_{y_O}}{\sqrt{\lambda^{*2}_{x_O} + \lambda^{*2}_{y_O}}}\right) \tag{12}$$

B. Transversality Conditions

Next we consider the transversality conditions which may be used to formulate the relationship between the states and costates at final time:

$$\frac{\partial h}{\partial \mathbf{x}}(\mathbf{x}^*(t_f), t_f) - \lambda^*(t_f) = d\frac{\partial m}{\partial \mathbf{x}}(\mathbf{x}^*(t_f), t_f) \tag{13}$$

We define $h(\mathbf{x}(t_f), t_f)$ as is the terminal cost of the objective functional, $\lambda(t_f)$ as the costates at final time, d as a slack variable, and $m(\mathbf{x}(t_f), t_f)$ as the terminal manifold. From (4), the terminal cost in the objective cost functional is constant, $\frac{\partial h}{\partial \mathbf{x}} = 0$. We defined the terminal manifold in (3) and therefore:

$$\begin{aligned} m(\mathbf{x}^*(t_f), t_f) = &\left(x^*_O(t_f) - x^*_T(t_f)\right)^2 \\ &+ \left(y^*_O(t_f) - y^*_T(t_f)\right)^2 - R^2 \end{aligned} \tag{14}$$

Substitution of (14) in to the transversality condition (13) we obtain the following:

$$-\lambda^*(t_f) = d\begin{bmatrix} \frac{\partial m}{\partial x_T} & \frac{\partial m}{\partial y_T} & \frac{\partial m}{\partial x_O} & \frac{\partial m}{\partial y_O} \end{bmatrix}^T \tag{15}$$

Therefore:

$$\lambda^*_{x_T} = \frac{\partial m}{\partial x_T} = 2d(x_O - x_T) \tag{16a}$$

$$\lambda^*_{y_T} = \frac{\partial m}{\partial y_T} = 2d(y_O - y_T) \tag{16b}$$

$$\lambda^*_{x_O} = \frac{\partial m}{\partial x_O} = 2d(x_T - x_O) \tag{16c}$$

$$\lambda^*_{y_O} = \frac{\partial m}{\partial y_O} = 2d(y_T - y_O) \tag{16d}$$

Taking the square root of (10) and substituting the costates from (16) we obtain the following:

$$\sin\psi^*(t_f) = \frac{\pm 2d(y_{T_f} - y_{O_f})}{\sqrt{4d^2(x_{T_f} - x_{O_f})^2 + 4d^2(y_{T_f} - y_{O_f})^2}} \tag{17}$$

Simplifying (17), we obtain a relationship between the states of the observer and target at the final time, t_f:

$$\sin\psi^*(t_f) = \frac{\pm(y_{T_f} - y_{O_f})}{R} \tag{18}$$

From (18) we see that the angle from the observer to the target at final time is the same as the optimal heading. An illustration of the optimal engagement is shown in Fig. 2.

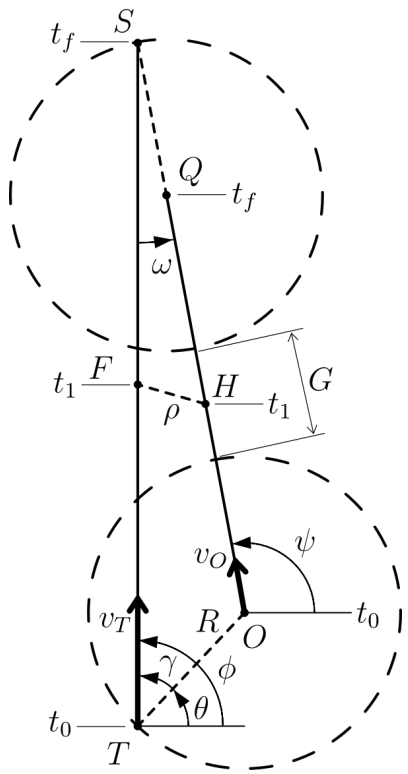

Fig. 2. Optimal Two Agent Engagement Geometry

III. Main Result

Knowing the course of the target, the optimal heading of the observer which maximizes the time of observation may be analytically obtained. Without loss of generality, the observer-target scenario is rotated about the target such that the target velocity is aligned with the vertical axis as shown in Fig. 2.

A. Optimal Observer Heading

The necessary conditions of optimality (7) have shown that optimal headings are constant (12). The transversality conditions (13) have shown that the angle from the observer to the target at final time is the same as the optimal heading (18). Using the law of cosines, the optimal heading of the observer may be obtained.

Theorem 1: The optimal heading of the observer which maximizes observation time is: $\psi^* = \cos^{-1}\left(\frac{(\alpha^2-1)\sin\gamma}{\alpha^2+2\alpha\cos\gamma+1}\right)$; where $\alpha \in (0,1)$ is the speed ratio and $\gamma \in [-\pi, \pi]$ is the bearing from the target to the observer.

Proof: Using the law of cosines for the triangle, $\triangle OST$:

$$\overline{OS}^2 = \overline{TS}^2 + R^2 - 2R\overline{TS}\cos\gamma \tag{19}$$

Utilizing the speed ratio, the distance traversed by the target is the same as α multiplied by the distance traversed by the observer and therefore:

$$\overline{OS} = \alpha\overline{TS} + R \tag{20}$$

Substituting (20) into (19):

$$(\alpha\overline{TS} + R)^2 = \overline{TS}^2 + R^2 - 2R\overline{TS}\cos\gamma \tag{21}$$

Expanding (21):

$$\alpha^2\overline{TS}^2 + R^2 + 2\alpha R\overline{TS} = \overline{TS}^2 + R^2 - 2R\overline{TS}\cos\gamma \tag{22}$$

Canceling R^2 terms on either side of the equals sign in (22) the following is obtained:

$$\alpha^2\overline{TS}^2 + 2\alpha R\overline{TS} = \overline{TS}^2 - 2R\overline{TS}\cos\gamma \tag{23}$$

Dividing both sides of (23) by $\overline{TS}$:

$$\alpha^2\overline{TS} + 2\alpha R = \overline{TS} - 2R\cos\gamma \tag{24}$$

Solving (24) for $\overline{TS}$ a formulation for the observed time is obtained as a function of the exposure radius, R, speed ratio α and initial target-observer angle, γ:

$$\overline{TS} = \frac{2R(\alpha + \cos\gamma)}{1-\alpha^2} \tag{25}$$

Since the cosine of an angle is the adjacent distance over the hypotenuse, the following is obtained:

$$\cos(\pi - \psi) = \frac{R\sin\gamma}{\alpha\overline{TS} + R} \tag{26}$$

We may substitute (25) into (26) and therefore

$$-\cos\psi = \frac{R\sin\gamma}{\alpha\frac{2R(\alpha+\cos\gamma)}{1-\alpha^2} + R} \tag{27}$$

Through algebraic manipulation of (27) one obtains the optimal observer heading

$$\psi^* = \cos^{-1}\left(\frac{(\alpha^2-1)\sin\gamma}{\alpha^2+2\alpha\cos\gamma+1}\right) \tag{28}$$

■

Special Case: $\gamma = 0$

When the angle of approach, γ, is zero, we see from (28) that the speed ratio does not come into play and the optimal heading of the observer is $\psi = \pi/2$ as expected.

Invariance of Observation Range

Next, we show that once the observer is within a range, R, of the target, under optimal play, the target remains within the observation range until the termination set is reached. Fig. 2 describes the geometry for the optimal two-agent scenario.

Theorem 2: $\rho < R \; \forall \; t \in (t_0, t_f)$, where ρ is the observer-target range at any time from the open interval starting at t_0 and ending at t_f.

Proof: Utilizing the Law of Cosines to analyze $\triangle OST$ we obtain the following relationship:

$$\overline{TO}^2 = \overline{TS}^2 + (\overline{OQ} + \overline{QS})^2 - 2\overline{TS}(\overline{OQ} + \overline{QS})\cos\omega \tag{29}$$

We recognize that $\overline{OT} = R$, $\overline{QS} = R$, and $\overline{TS} = \alpha\overline{OQ}$. Substitution into (29), we obtain:

$$R^2 = \overline{TS}^2 + (\alpha\overline{TS} + R)^2 - 2\overline{TS}(\alpha\overline{TS} + R)\cos\omega \tag{30}$$

Expanding and solving (30) for $\cos\omega$:

$$\cos\omega = \frac{\overline{TS}(1+\alpha) + 2\alpha R}{2(\alpha\overline{TS} + R)} \tag{31}$$

Now consider a future time, $t_1 \in (t_0, t_f)$. Using the Law of Cosines for $\triangle FHS$:

$$\rho^2 = \overline{FS}^2 + \overline{HS}^2 - 2\overline{FS}\,\overline{HS}cos\omega \tag{32}$$

We recognize that $\overline{HQ} = \alpha\overline{FS}$ and $\overline{HS} = \overline{HQ} + R$. Substituting these into (32):

$$\rho^2 = \overline{FS}^2 + (\alpha\overline{FS} + R)^2 - 2\overline{FS}(\alpha\overline{FS} + R)cos\omega \tag{33}$$

Substituting (31) into (33):

$$\begin{aligned}\rho^2 =& \overline{FS}^2 + (\alpha\overline{FS} + R)^2 \\ &- 2\overline{FS}(\alpha\overline{FS} + R)\frac{\overline{TS}(1+\alpha) + 2\alpha R}{2(\alpha\overline{TS} + R)}\end{aligned} \tag{34}$$

Manipulating (34):

$$\rho^2 = R^2 + \frac{\overline{FS}R}{(\alpha\overline{TS} + R)}\left(\overline{FS} - \overline{TS}\right)\left(1 - \alpha^2\right) \tag{35}$$

Notice in (35)

$$\rho^2 = R^2 + \underbrace{\frac{\overline{FS}R}{(\alpha\overline{TS} + R)}}_{\text{Positive}}\underbrace{\left(\overline{FS} - \overline{TS}\right)}_{\text{Negative}}\underbrace{\left(1 - \alpha^2\right)}_{\text{Positive}} \tag{36}$$

Therefore, for values of $t_1 \in (t_0, t_f)$, $\rho < R$.

■

B. Observation Limaçon

The function which describes the target distance while being observed can be found in (25). The target distance while being observed is a function of the bearing from the target to the observer, γ; the radius of observation, R; and speed ratio, α. Because we normalize the velocity with respect to the target vehicle, the range $\overline{TS} = v_T t = t$. Substituting the time of exposure, t into (25) the polar equation for exposure time is the following:

$$t_f = \frac{2R(\alpha + \cos\gamma)}{1-\alpha^2} \tag{37}$$

Plotting the time of exposure as a function of the target to the observer, γ, produces a limaçon whose cusp is located at the target location. Utilizing (37), we derive the angle which describes the range of headings the target could take which result in a zero-observation time (ZOT). Note that zero-time of exposure solutions exist when $t_f = 0$. From (37), values of γ which result in non-positive values of t_f represent angles for which the observation time is zero. Thus, setting the length $t_f \leq 0$, we find from (37):

$$\frac{2R}{1-\alpha^2}(\alpha + \cos\gamma) \leq 0 \tag{38}$$

From (38), we find the regions where the observer is unable to observe the target occurs when the angle γ lies in the following range:

$$\gamma_{ZOT} \in [\cos^{-1}(-\alpha), \pi] \cup [-\pi, -\cos^{-1}(-\alpha)] \tag{39}$$

Assuming the observer implements the optimal heading which maximized observation time of the faster target, eq. (25) can be algebraically manipulated to provide the observer-target headings which guarantee a desired observation time. The following is the equation which describes the angle γ which guarantees the desired observation time, t.

$$\gamma = \cos^{-1}\left(\frac{(1-\alpha^2)t - 2\alpha R}{2R}\right) \tag{40}$$

It should be noted that the guarantees for observation time are bounded by

$$t \in \left[0, \frac{2R(\alpha+1)}{1-\alpha^2}\right] \tag{41}$$

IV. Example

Consider the scenario with capture radius, $R = 1.00$; speed ratio, $\alpha = 0.8$; target's constant heading, $\phi = \pi/2$ rad; and target-observer angle, $\gamma = 7/18\pi$ rad. Utilizing (28), the optimal observer heading, ψ^* is computed and is ≈ 1.726 rad. Utilizing the calculated optimal observer heading, the max-time observation of a faster target can be seen in Fig. 3. In the figure, the observer is represented by the blue line, the observation radius is represented by the dashed line, and the faster target is represented by the red line.

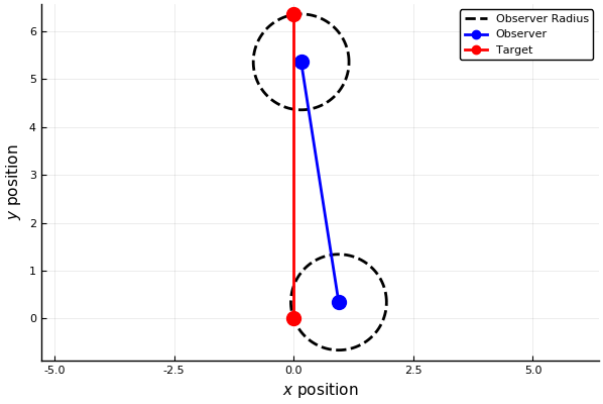

Fig. 3. Observation Scenario

For the scenario described in Fig. 3, consider the observer-target range throughout the engagement. In Theorem 2 we showed that the observer-target range remains less than the observer range under optimal play. In Fig. 4, the observer range is represented by the dashed black line and the instantaneous observer-target range is represented by the solid black line. As we have predicted, the observer-target range remains less than the observer range for the entire engagement, as required.

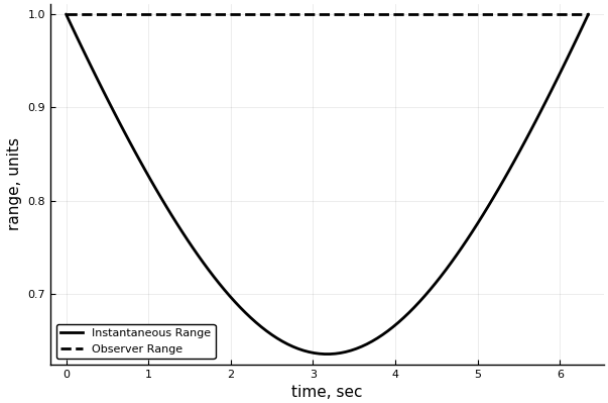

Fig. 4. Scenario Observation Range

Next, consider arbitrary observer-target aspect angles: $\gamma \in [-\pi, \pi]$. In the event that the observer selects the optimal heading described by (28), the time of observation may be computed using (37). In Fig. 5 the optimal observation time is found for arbitrary aspect angles, γ. From the figure, the blue line represents all cases where the observer is able to observe the target for a non-zero amount of time. The green line represents the computed observation time from (37). While the negative values signify that the observer is unable to observer the target for any amount of time. The green dot designates the angle γ_{ZOT} for which there is zero observation time. Finally, the black dot is the computed maximum observation time, which occurs when $\gamma = 0$.

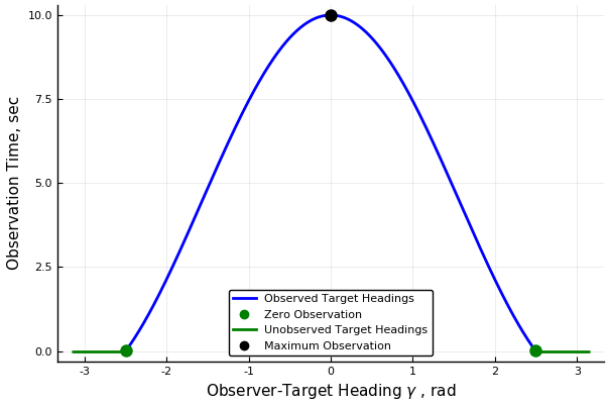

Fig. 5. Time of observation of the Evader by the Pursuer

A plot which describes the observation time for arbitrary observer-target headings was shown in Fig. 5. However, how

this relates to an actual engagement scenario may be unclear. Plotting the observation time in a polar sense for each aspect angle, γ, the limaçon which describes the observed time for each aspect angle, γ, can be seen in Fig. 6. In the figure, the blue shaded region represents the region of observability of the target by the observer for all possible observer-target headings. The green region represents the target headings for which the observer would have no observation of the faster target. Considering, the scenario in our example, the red line represents the course taken by the target, the blue line represents the observer under optimal play, and the dotted black lines represent the observer's range at the beginning and end of the engagement.

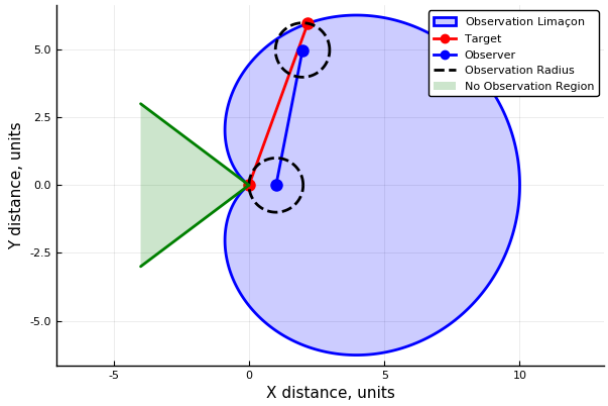

Fig. 6. Observation Limaçon and Zero-Observation Region

V. Conclusions

Using a circular observation region centered at the observer and commanding the instantaneous heading of the observer, we maximized the time by which the target remains inside the observation range. Utilizing the theory of optimal control, we have posed and solved for the optimal instantaneous observer heading required to maximize the observation of a faster but non-maneuvering target. We showed the heading which maximizes the time of observation is constant. Further, the optimal heading is only dependent upon the relative bearing of the target to the observer as well as the speed ratio parameter. Next, we showed that no intermittent contact occurs under optimal control, e.g. the observation range is less than the radius of observation for the entire engagement. Finally, we present the observation time as a function of observer-target aspect angle. Plotting the observation time as a function of the observer-target aspect angle, we found the limaçon describing target observation time. Utilizing the limaçon we were able to illustrate the target observation based upon the target's bearing.

References

[1] Z. S. Wowczuk, E. D. Pertl, M. A. Clarke, J. E. Smith, S. Bjorge, and R. McNutt, "Complete Command, Control, Communications, Intelligence, Surveillance, and Reconaissance System for C-130 Aircraft," *Journal of Aerospace Computing, Information, and Communication*, vol. 7, no. 6, pp. 179–187, 2010.

[2] D. J. Henry, "ISR Systems: Past, Present, and Future," in *Airborne Intelligence, Surveillance, Reconnaissance (ISR) Systems and Applications XIII*, vol. 9828, (Baltimore, MD), p. 982802, SPIE, 2016.

[3] B. M. Kent and R. A. Ehret, "Rethinking Intelligence, Surveillance, and Reconnaissance in a Wireless Connected World," in *IEEE Antennas and Propagation Society, AP-S International Symposium (Digest)*, (Chicago, IL), p. 2, IEEE, 2012.

[4] M. Wilkins and T. Marchelli, "An Optimal Approach to Unmanned Maritime Surveillance Analysis," in *12th AIAA/ISSMO Multidisciplinary Analysis and Optimization Conference*, (Victoria, British Columbia, Canada), pp. 1–7, American Institute of Aeronautics and Astronautics (AIAA), 2012.

[5] R. He, A. Bachrach, and N. Roy, "Efficient Planning Under Uncertainty for a Target-Tracking Micro-Aerial Vehicle," in *Proceedings - IEEE International Conference on Robotics and Automation*, (Anchorage, AK), pp. 1–8, IEEE, 2010.

[6] R. A. Livermore, "Optimal UAV Path Planning for Tracking a Moving Ground Vehicle With a Gimbaled Camera.," pp. 1–106, M.S. Thesis. Air Force Institute of Technology, 2014.

[7] M. Wohlsen, "The Ex-Googlers Building Drones that Anybody can Pilot With a Phone," 2015.

[8] D. W. Oyler, *Contributions to Pursuit-Evasion Game Theory*. PhD thesis, University of Michigan, 2016.

[9] T. A. Wettergren and C. M. Traweek, "The Search Benefits of Autonomous Mobility in Distributed Sensor Networks," *International Journal of Distributed Sensor Networks*, vol. 2012, no. 2, p. 11, 2012.

[10] B. Liu, O. Dousse, P. Nain, and D. Towsley, "Dynamic Coverage of Mobile Sensor Networks," *IEEE Transactions on Parallel and Distributed Systems*, vol. 24, no. 2, pp. 301–311, 2013.

[11] J. M. Dobbie, "Solution of Some Surveillance-Evasion Problems by Methids of Differential Games," in *Proceedings of the 4th International Conference on Operational Research, MIT*, (New York, New York), pp. 170–184, John Wiley and Sons, 1966.

[12] J. G. Taylor, "Application of Differential Games to Problems of Naval Warware: Surveillance-Evasion - Part 1," tech. rep., United States Naval Postgraduate School, Monterey, CA, 1970.

[13] J. Lewin and J. V. Breakwell, "The Surveillance-Evasion Game of Degree," *Journal of Optimization Theory and Applications*, vol. 16, no. 3-4, pp. 339–353, 1975.

[14] J. Lewin and G. J. Olsder, "Conic Surveillance Evasion," *Journal of Optimization Theory and Applications*, vol. 27, no. 1, pp. 107–125, 1979.

[15] Z. E. Fuchs and J. Metcalf, "Equilibrium Radar-Target Interactions in an ATR Scenario: A Differential Game," in *2018 IEEE Radar Conference, RadarConf 2018*, (Oklahoma City, OK), pp. 1228–1233, IEEE, 2018.

[16] V. Patsko, S. Kumkov, and V. Turova, "Pursuit-Evasion Games," in *Handbook of Dynamic Game Theory* (Z. G. Basar T., ed.), pp. 1–87, Springer, Cham, 2018.

[17] R. J. Garnett and A. Flenner, "Optimal Control for Improved UAV Communication," in *AIAA Scitech Forum*, (San Diego, CA), pp. 1–14, American Institute of Aeronautics and Astronautics (AIAA), 2019.

[18] J. V. Breakwell, "Pursuit of a Faster Evader," in *The Theory and Application of Differential Games* (J. D. Grote, ed.), pp. 243–256, Springer, Dordrecht, 1975.

[19] D. E. Kirk, *Optimal Control Theory: An Introduction*. Dover Books on Electrical Engineering Series, Dover Publications, 2004.

[20] R. Isaacs, *Differential Games*. John Wiley and Sons, 1965.